Optical spectra of periodically patterned dielectric surface simulated by finite-different time-domain method

Journal of Physics: Conference Series **1380** (2019) 012151 doi:10.1088/1742-6596/1380/1/012151

Optical spectra of periodically patterned dielectric surface simulated by finite-different time-domain method

N Sitpathom[1], J M Dawes[2], T Muangnapoh[3], P Kumnorkaew[3], S Suwana[1], A Sinsarp[1] and T Osotchan[1]

[1]Department of Physics, Faculty of Science, Mahidol University, Bangkok 10400, Thailand
[2]Department of Physics and Astronomy, Faculty of Science and Engineering, Macquarie University, Sydney, NSW 2109, Australia
[3]Nanohybrid and Coating Research Group, National Nanotechnology Center, National Science and Technology Development Agency, Khlong Luang 12120, Thailand

E-mail: nonthanan.sit@student.mahidol.ac.th

Abstract. A dielectric film imprinted with a hexagonal periodical pattern of nanosphere holes can be fabricated by a two-step process of depositing a dielectric thin film on a hexagonally patterned array of nanospheres fabricated by convective deposition, and then removing the nanosphere particles. In this work, the optical transmission through a dielectric slab with hexagonal pattern of half-sphere holes was simulated by finite-different time-domain (FDTD) methods. In the simulation, a short gaussian pulse of electromagnetic waves was generated and propagated through the dielectric patterned slab and the near-field diffraction from the structure was collected as a function of time. Using a Fourier transformation, the optical spectra of the structure were evaluated. The far-field diffraction was also investigated by evaluating the analytical Green's function at given points. Several parameters of the optical response including full width at half maximum and relative intensities of high order diffraction peaks were examined for various structure sizes. The structures examined were composed of a periodic hexagonal pattern of half nanosphere holes (radius of 290 nm). In addition, the effect on the optical response of 10% elliptical shape deformation of the half-sphere holes was studied. Our calculations enable us to identify parameter schemes where the third order diffraction exceeds second order diffraction efficiency from gratings.

1. Introduction

Gratings are useful for many applications such as tuneable colour filters [1], chemical sensors [2], strain sensors [3] or thermal sensors [4]. Sensing by gratings is performed by detecting reflected or transmitted optical diffraction as a function of the change in the grating period. Optical gratings can be fabricated in two dimensions with photoresist polymer by lithography [5] or in one dimension by fabricating Bragg gratings in fibre optics for pressure sensing [6]. In addition, two-dimensional gratings can be simply created by patterning a self-assembled array onto a flexible polymer film [7].

The grating shape and duty cycle affect the grating efficiency, which is given by the ratio between diffracted and incident powers. For certain specific conditions of the grating duty cycle, the fraction of on-and-off cycle, the power of the third diffraction order can be stronger than that of the second order

[8]. Additionally, the choice of grating shape (for example an echelle grating with different groove shape [9]), can also affect the efficiency at particular wavelengths.

Although the grating efficiency for simple structures may be derived by analytic approaches, the solution for complicated grating structures may need numerical models. The efficiency of diffraction from coated gratings with complex shape or imperfect gratings can be derived numerically, by finite-different time-domain (FDTD) methods.

Near-field or Fresnel diffraction is affected by the Talbot effect [10]. To reduce the Talbot effect, the near-field diffraction must be transformed to the far field [11].

In this work, the optical diffraction from semi-holes on dielectric films was studied by FDTD. An optical power spectrum as a function of the transmitted angle with normal incidence was investigated by transforming the near-field to far-field diffraction by Greens function. The grating diffraction strength compared between other diffracted orders was investigated with variations of the grating period and shape.

2. Simulation

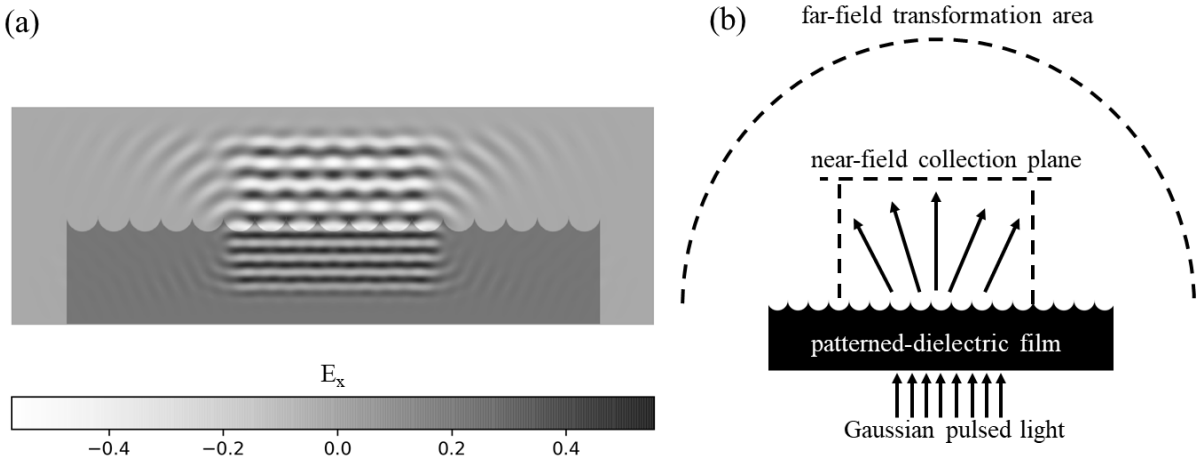

Figure 1. (a) computed model of dielectric film with curvature hole shown in E_x field and (b) diagram of far-field transformation from near-field collection plane.

Dielectric gratings were simulated in two dimensions by finite-different time-domain with finite structure. Simulation with finite-different time-domain (FDTD) was performed by the MEEP open-software, which has been developed by a team at Massachusetts Institute of Technology. A plane source generated Gaussian pulsed waves with E_x polarization and bandwidth of 5.8×10^{15} Hz. The incident waves propagated from the un-patterned side as seen in figure 1. The diffracted waves (electric and magnetic fields) were collected by three defined lines as a time series and the collected fields were Fourier transformed. The Fourier-transformed data over the near-field region was input to the Green's function [12], and the diffracted fields at far field region were computed that were seen in equation (1) and equation (2).

$$\vec{E}(\vec{r}) = \oiint_{s'} \{i\omega\mu \overline{\overline{G}}(\vec{r},\vec{r}') \cdot [\hat{n} \times \vec{H}(\vec{r})] + \nabla \times \overline{\overline{G}}(\vec{r},\vec{r}') \cdot [\hat{n} \times \vec{E}(\vec{r})]\} ds' \quad (1)$$

$$\vec{H}(\vec{r}) = \oiint_{s'} \{i\omega\mu \overline{\overline{G}}(\vec{r},\vec{r}') \cdot [\vec{E}(\vec{r}) \times \hat{n}] + \nabla \times \overline{\overline{G}}(\vec{r},\vec{r}') \cdot [\hat{n} \times \vec{H}(\vec{r})]\} ds' \quad (2)$$

where

$$\overline{\overline{G}}(\vec{r},\vec{r}') = (\overline{\overline{I}} + \frac{1}{k^2}\nabla\nabla)\frac{e^{ik|\vec{r}-\vec{r}'|}}{4\pi|\vec{r}-\vec{r}'|}$$

is the dyadic Green's function.

The far field spectrum was investigated in a hemi circle with radius of 1000 times the wavelength of 400 nm. The computed structure was a finite structure with 15 periods. The structure was surrounded by perfect-matched layers (PML) with thickness of 1 μm to prevent waves reflecting from the computation cell. The three lines (dash lines) above the patterned surface accumulated electric and magnetic fields until the electric field decayed to 10^{-10} times that of the initial field. The collection time was sufficiently long to completely gather the time-series field.

The diffraction spectrum at the far-field diffraction region was studied for various period distances and curvature shapes. The far-field diffraction spectrum was described in terms of the optical power by Poynting's theorem, Re{E*(r)xH(r)}. The period distance was varied from 580 nm to1595 nm (2.75d). Moreover, the transmitted diffraction was considered for the shape with the circle hole shifted to 150 nm above the film. The curvature shape was deformed from a perfect circle to an ellipse with lengths of minor axis as 240 nm, 190 nm and 140 nm.

3. Results and discussion

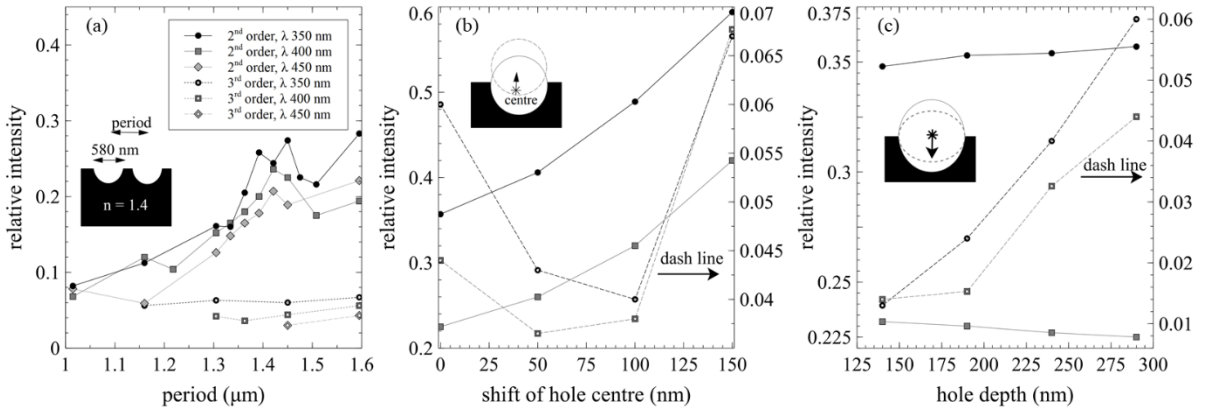

Figure 2. Relative intensities of the second diffraction order to the first and the third order to the first affected by (a) period change, (b) shifted centre of hole and (c) depth of hole shown in wavelengths of 350 nm, 400 nm and 450 nm.

Diffraction at the far field can be numerically calculated by the Green's function and Fourier transformation. The near-field diffraction from a dielectric film with refractive index of 1.4, patterned with semi-circle holes is shown in figure 1 (a) for a wavelength of 400 nm with electric polarization in x-direction.

The power spectra of the first order diffraction were evaluated at varied period with fixed diameter of hemisphere hole at 580 nm on top of surface. The diffraction respective to incidence powers of the zero order diffraction for period values of 580, 870, 1160 and 1450 nm are 0.05, 0.25, 0.27, and 0.25, moreover, these diffraction peaks occurred at the angle of 43°, 27°, 20° and 16°, respectively. The effect of the duty cycle of the curved grating on the strength of various diffraction orders was studied, with periods of 1015 nm to 1595 nm and at wavelengths of 350 nm, 400 nm and 450 nm. The relative intensity of the diffracted wavelengths between the second order and the first order are shown in figure 2 (a). In this figure the relative intensities of the third diffraction order to the first diffraction order for various periods are illustrated. For the wavelength of 350 nm, the relative intensities of the second order and the first order continuously increased until achieving the highest ratio of 0.357 at a period of 1450 nm, and it reduced for a period of 1595 nm. This trend was similar to that for a wavelength of 400 nm, but there was a peak of ratio at a period of 1305 nm with a ratio of 0.306. However, the trend for the diffraction

of 450 nm contrasted to the others. There was a minimum at a relative intensity of 0.059 with a period of 1160 nm, and the second order to first order diffraction ratio increased after this.

The effect of shifting the air-hole upwards 50 nm, 100 nm and 150 nm, over the dielectric surface is shown in figure 2 (b) while the period was fixed to 1.45 μm. The ratio of intensities of the second order to the first order diffraction increased for both wavelengths of 350 nm and 400 nm when the air-hole centre was lifted above the initial position. In contrast to the ratio of the third order to the first, there was a similar trend for wavelengths of 350 nm and 400 nm when the hole centre shifted from the initial position. Changing the centre of the air hole had an effect on both the grating depth and period length, so both parameters influenced the observed behaviour.

Finally, the dependence on grating shapes was studied by changing the circular curve to an ellipsoidal curve. The circular shape over the film at period of 1.45 μm was deformed to an ellipse with minor axis of 290 nm, 240 nm, 190 nm and 140 nm, and the major axis, parallel to the surface, remained the same. The far-field diffraction of this case was shown in figure 2 (c). The relative intensities of the second order to the first order slightly increased and decreased for wavelengths of 350 nm and 400 nm, respectively. Changes in the pattern depth made small effects on the relative intensity, so the effect of pattern depth appears weaker than the effect of period length.

4. Conclusion

The optical strength of diffraction was affected by the grating period. Moreover, the intensity of the second order can approach that of the first order when the centre of the holes is shifted above the film surface. Nevertheless, the relative intensity of the second diffraction order to the first was only slightly affected when the grating shape was deformed to an ellipse because the fill factor was unchanged.

Acknowledgments

This work was partially supported by the National Nanotechnology Center (NANOTEC) through Research Nanotechnology network (RNN).

References

[1] Cho H, Han S, Kwon J, Jung J, Kim H J, Kim H, Eom H, Hong S and Ko S H 2018 *Opt. Lett.* **43** 3501–4
[2] Wang X, Ye G and Wang X 2014 *Sens. Actuators B Chem.* **193** 413–9
[3] Guo H, Tang J, Qian K, Tsoukalas D, Zhao M, Yang J, Zhang B, Chou X, Liu J, Xue Ch and Zhang W 2016 *Sci. Rep.* **6** 23606
[4] Sharac N, Sharma H, M Veysi, Sanderson R N, Khine M, Capolino F and Ragan R 2016 *Nanotechnology* **27** 105302
[5] Zhang X, Zhang J, Liu H, Su X and Wang Li 2014 *Sci. Rep.* **4** 4182
[6] Liang M F, Fang X Q, Wu G, Xue G Zh and Li H W 2017 *Optik* **145** 503–12
[7] Piccolo V, Chiappini A, Armellini C, Barozzi M, Lukowiak A, Sazio P-J A, Vaccari A, Ferrari M and Zonta D 2018 *Micromachines* **9** 345
[8] Shih W-C, Kim S-G and Barbastathis G 2006 *J. Microelectromech. S.* **15** 763–9
[9] Zhang Sh, Mi X, Zhang Q, Jirigalantu, Feng Sh, Yu H and Qi X 2017 *Opt. Commun.* **387** 401–4
[10] Bělín J and Tyc T 2018 *J. Opt.* **20** 025604
[11] Zhai P-W, Lee Y-K, Kattawar G W and Yang P 2004 *Appl. Opt.* **43** 3738–46
[12] Li P and Jiang L J 2012 *Prog. Electromagn. Res.* **123** 243–61